Supporting information

In-situ construction of donor-acceptor structured g-C_3N_4 nanotubes incorporated with pyridine heterocyclic rings for efficient photocatalytic water splitting

Bo Zhang[a], Wenjing Luo[a], Luye Pan[a], Chenhuan Tian[b], Peipei Sun[a], Pengcheng Yan[a,*], Xianglin Zhu[a], Haibo Wang[c,*], Zhao Mo[a,*], Hui Xu[a]

[a] School of Materials Science & Engineering, School of the Environment and Safety Engineering, Institute for Energy Research, Jiangsu University, Zhenjiang 212013, P. R. China

[b] School of Foreign Languages, Southeast University, Nanjing 211189, P. R. China

[c] Jiangsu Vocational College of Electronics and Information, Huaian 223003, P. R. China

*Corresponding author e-mail address: yanpengcheng@ujs.edu.cn; whb@jsei.edu.cn; zhaomo@ujs.edu.cn

1. Experimental Part

1.1 Reagent characterization

Melamine ($C_3H_6N_6$, 98%), nicotinic acid ($C_6H_5NO_2$, 99%), ethanol (C_2H_5OH, 99%), triethanolamine (TEOA, 99%), chloroplatinic acid ($H_2PtCl_6 \cdot 6H2O$, 99%) and other chemicals were commercially available analytical products purchased from Zhongke Chemical Reagent Co., Ltd. (Shanghai, China) without any further pretreatment.

1.2 Preparation of photocatalytic materials

The preparation method of the PCN material is as follows: 1 g of melamine was poured into a crucible and placed in a muffle furnace for calcination. The calcination conditions involved raising the temperature inside the muffle furnace from room temperature to 500 °C at a heating rate of 2 °C/min, and maintaining the high temperature of 500 °C for 4 h. After calcination, a yellow block sample was cooled down to room temperature. Subsequently, the sample was thoroughly ground into fine powder for future use.

The preparation method of NA_X-CN material is as follows: 2 g melamine and X (X = 50, 100 and 150 mg) nicotinic acid were sequentially dispersed in 35 mL of deionized water in turn, and the dispersed mixed solution was put into 50 mL of Teflon-lined autoclave for hydrothermal reaction in oven at 200 ℃. After the reaction, the solids were collected by centrifugation and washed three times with deionized water and ethanol. Then, put the washed sample into a 60 °C drying oven for thorough drying to obtain white intermediates. 1 g intermediate was placed in a crucible and calcined at 500 °C for 4 h in a muffle furnace at a heating rate of 2 °C/min. The obtained fluffy light yellow powder was named NA_X-CN.

1.3 Material characterization

The as-prepared samples were analyzed by X-ray diffraction (XRD) by Bruker D8 diffractometer with Cu Kα radiation (λ=1.5418 Å) in the range of 2θ=10-80°. The structural information for samples was measured by Fourier transform infrared spectroscopy (FTIR, Avatar 470, Thermo Nicolet) using the standard KBr disk method. The morphology and structure of the samples were investigated with scanning electron microscope (SEM) and transmission electron microscopy (TEM). The SEM images were taken on a field-emission microscope by a JEOL JSM-7001F. The transmission electron microscopy (TEM) images were collected with a JEOL-JEM-2010 (JEOL, Japan) operated at 200 kV. Elemental compositions were detected by X-ray photoelectron spectroscopy (XPS) analysis which was performed on an ESCALab

MKII X-ray photo-electron spectrometer using the Mg Kα radiation. The Brunauer-Emmett-Teller (BET) specific surface area and average pore size distribution were measured using nitrogen (N_2) adsorption/desorption at 77 K on a TriStar II 3020. UV-visible (UV-Vis) absorption spectra were measured using a Shimadzu UV-2600i UV-Vis spectrophotometer, with a wavelength measurement range of 200-800 nm, using $BaSO_4$ as the reflection standard material. Steady-state fluorescence spectra were recorded using a Thermo Scientific Lumina instrument. Photoluminescence is measured by a QuantaMaster40 (Photon Technology International, USA) with an excitation wavelength of 360 nm at room temperature. Electrochemical impedance spectroscopy (EIS), photocurrent, polarization curves, Mott-Schottky plots, and cyclic voltammetry curves were measured on an electrochemical analyzer using a standard three-electrode configuration, with 0.5 mol/L Na_2SO_4 as the electrolyte, platinum wire as the counter electrode, fluorine-doped tin oxide (FTO) as the working electrode, and Ag/AgCl (saturated KCl) as the reference electrode. During the Photocurrent measurements, 1 mL of deionized water containing 1 mg of sample powder was uniformly dispersed in three parts using ultrasonic waves. Then, 50 μL of a colloidal dispersion with a concentration of 1 mg/mL was dropped onto an FTO substrate (with a fixed area of 0.5 cm^2). It was placed under an infrared lamp for drying to obtain a sample-modified FTO electrode. All photocurrent measurements were conducted at a constant potential of 0 V relative to Ag/AgCl in 0.1 M potassium chloride (KCl)and A 300 W Xe arc lamp was used as the light source. Using a 5 mM mixture of $K_3[Fe(CN)_6]$ and $K_4[Fe(CN)_6]$ (1:1) as the redox probe for EIS measurements. The electrolyte during photoelectrochemical tests is 0.1 M phosphate buffer (pH = 7.0).

1.4 Photocatalytic hydrogen evolution experiment

10 mL of triethanolamine, 90 mL of water, and 10 mg of catalyst were added to the reactor. Ultrasonic treatment was performed for 10 minutes to ensure uniform mixing. Then, 200 μL of 3% mass platinum chlorate Pt was added, and Pt is photo-deposited in situ on the surface of the catalyst to serve as a co-catalyst. The reactor was connected to the hydrogen evolution device. Magnetic stirrings were used to ensure uniform mixing of the liquid in the reactor, and circulate 10 °C constant temperature cooling water on the outer layer of the reactor. Photocatalytic HER activity was assessed using a fully automatic all-glass trace gas online analyzer (LbSolar-6A, Beijing PerfectLight) (**Fig. S1**). A 300 W xenon lamp with a wavelength of 400 nm served as the light source. The photocatalytic HER performance was measured by online gas chromatograph (GC

9700 II, TCD, FULI Instruments (**Fig. S2**)). The final hydrogen production amount of photocatalysis was analyzed by Ar carrier gas, a TCD detector, and 5Å molecular sieve. When finished one cycle, the sample would be washed by deionized water and anhydrous ethanol for several times, and then dried at 80°C overnight to remove the adsorbed TEOA on the surface.

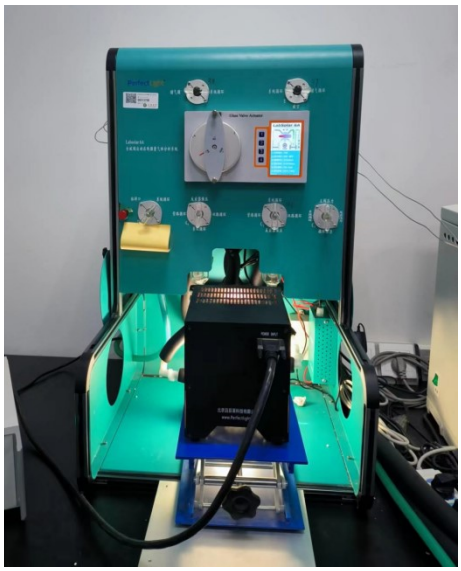

Fig. S1 The digital photo of the photocatalytic reactor used in this work.

Fig. S2 The digital photograph of the gas chromatography used in this work.

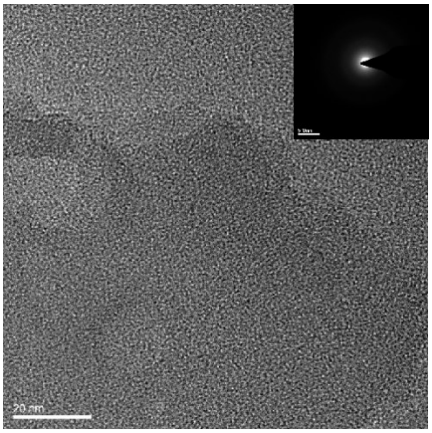

Fig. S3 Morphological analysis diagram of NA100-CN by high-resolution TEM.

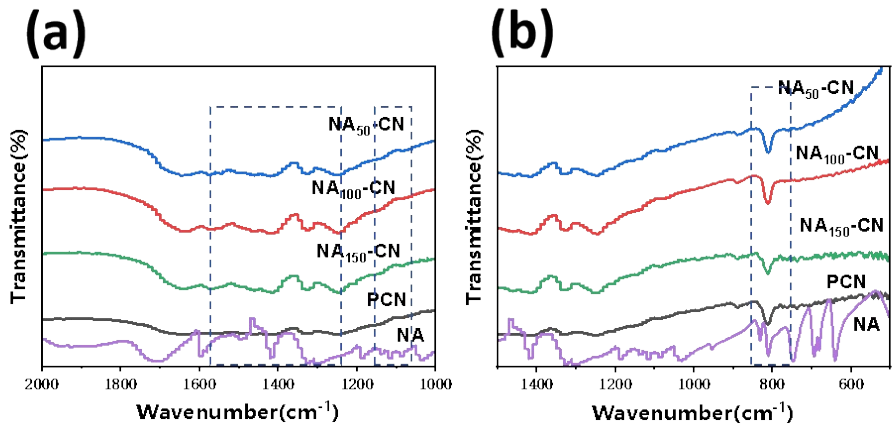

Fig. S4 FT-IR spectra of NA_X-CN, PCN and NA.

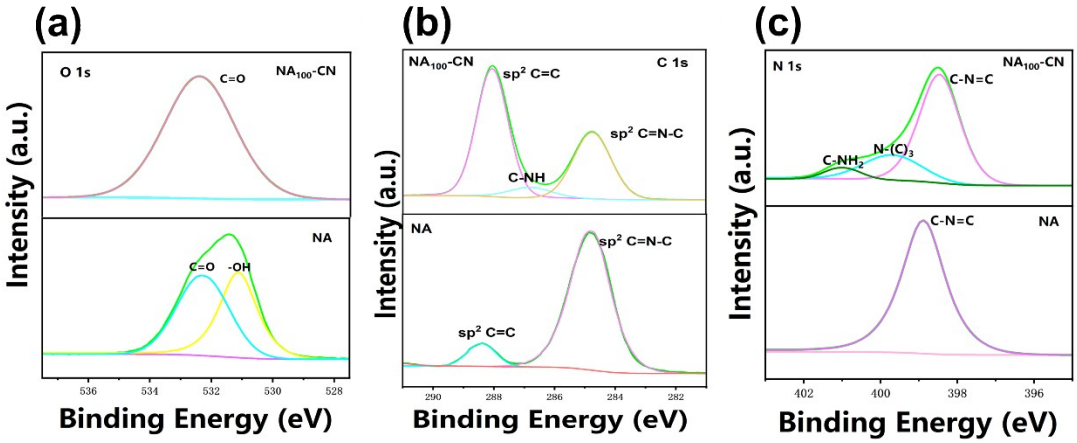

Fig. S5 (a) O 1s spectra (b) C 1s spectra, and (c) N 1s spectra of NA_{100}-CN and NA.

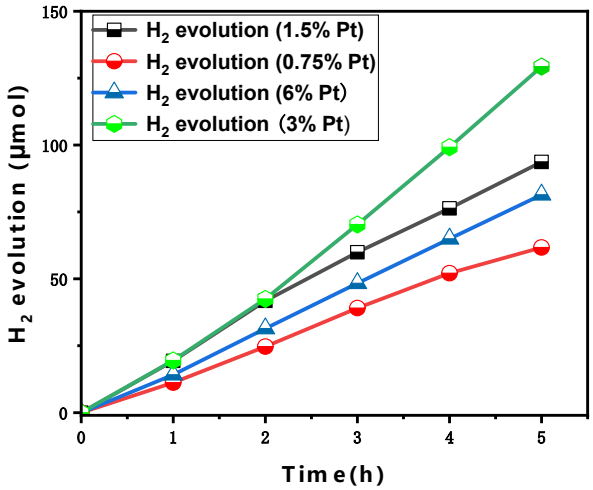

Fig. S6 The photocatalytic H_2 evolution of different Pt loading content over NA100-CN.

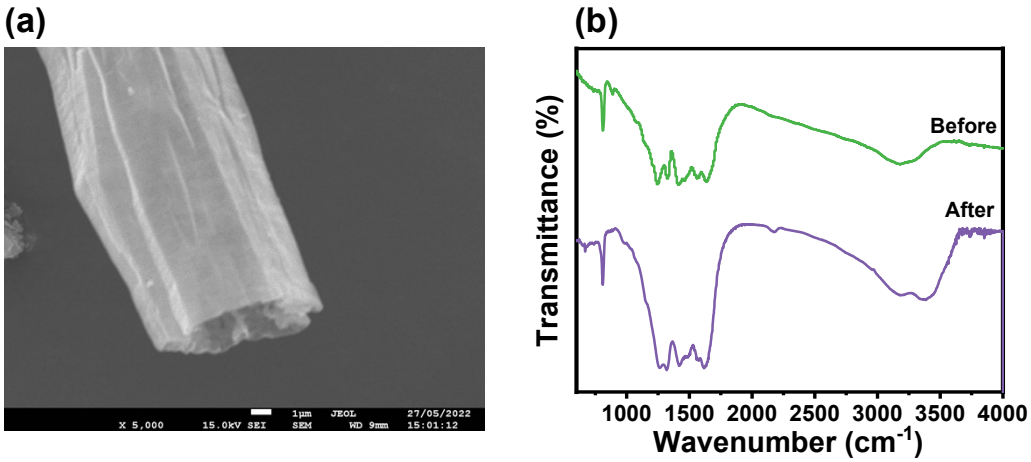

Fig. S7 SEM images and FT-IR spectra of NA_{100}-CN before and after 5 cycles.

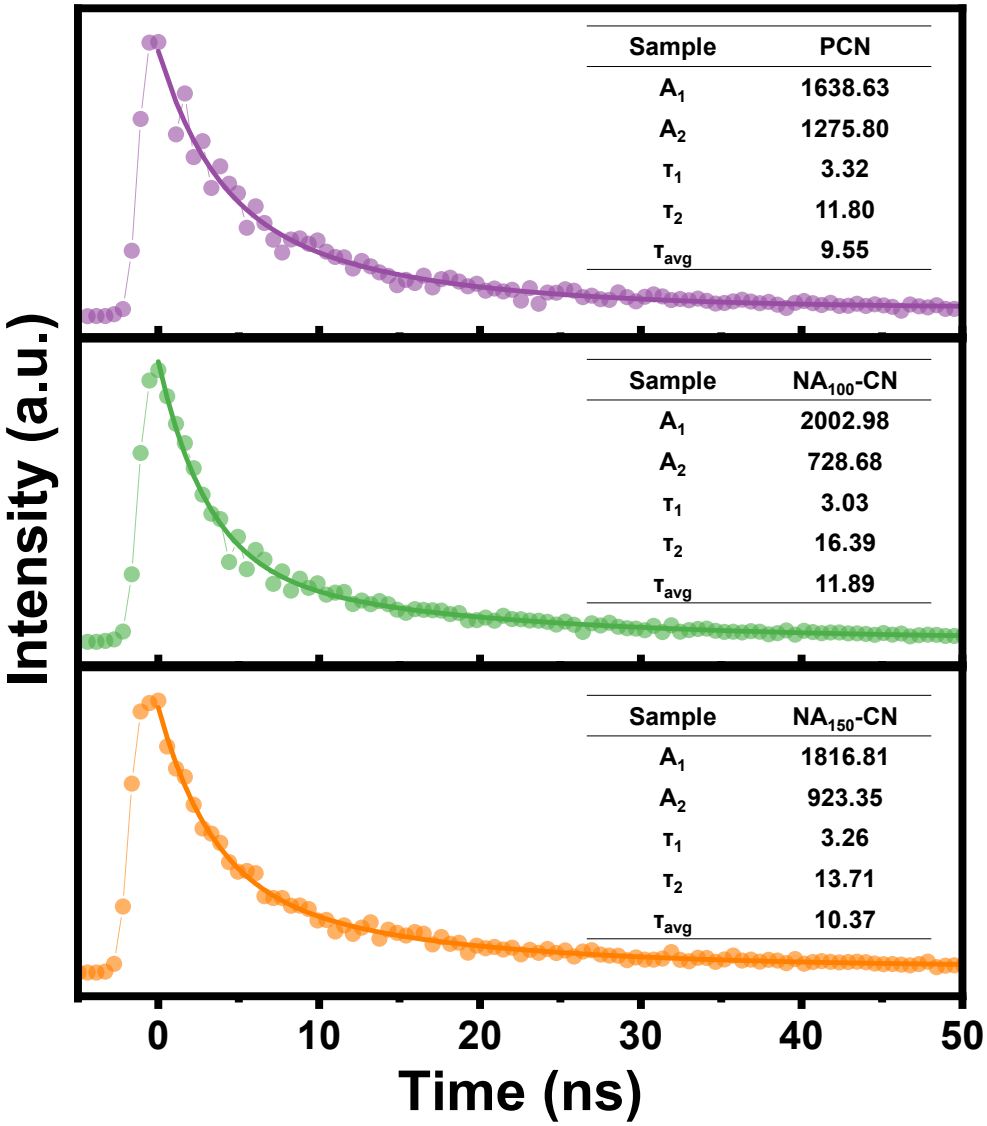

Fig. S8 Time-resolved PL spectra of PCN and NA100-CN.

Table S1 The percentage of the integrated area of each signal in the XPS C 1s.

Elements	Bond	PCN (%)	NA100-CN (%)
C 1s	N-C=N	85.20	57.61
	C-NH_x	4.41	6.82
	C=C	10.47	35.64
	C=C/N-C=N	0.12	0.61

Table S2 Elemental Analysis of PCN and NA_{100}-CN

	C(%)	N(%)	O(%)
PCN	33.24	59.57	7.384
NA_{100}-CN	33.41	60.40	8.012

Table S3 Summary of donor-acceptor structured g-C_3N_4 photocatalysts for photocatalytic H_2 evolution.

Photocatalyst	Light source	Reaction conditions	Hydrogen evolution	Ref.
$PTCN_6$	**300 W Xe lamp, λ > 400 nm**	**10 mg, 3 wt% of Pt co-catalyst, TEOA (10%)**	**2584.2 μmol h^{-1} g^{-1}**	**This work**
CUCN	300 W Xe lamp, λ > 420 nm	15 mg, 3 wt% of Pt co-catalyst, TEOA (10%)	2231.8 μmol h^{-1} g^{-1}	[1]
PTHCN-5	300 W Xe lamp, λ > 420 nm	50 mg, 1 wt% of Pt co-catalyst, TEOA (10%)	6640 μmol h^{-1} g^{-1}	[2]
g-CN/Crings	300 W Xe lamp, λ > 420 nm	20 mg, 0.5 wt% of Pt co-catalyst, TEOA (10%)	2390 μmol h^{-1} g^{-1}	[3]
TCN-MB_{10}	300 W Xe lamp, AM 1.5 G	20 mg, 3 wt% of Pt co-catalyst, TEOA (10%)	2275.6 μmol h^{-1} g^{-1}	[4]
CN_{urea}-$Ni(abt)_2$	300 W Xe lamp, λ > 420 nm	10 mg, TEOA (10%)	100 μmol h^{-1} g^{-1}	[5]
g-PAN/CN	300 W Xe lamp, λ > 400 nm	100 mg, 1.5 wt% of Pt co-catalyst, TEOA (10%)	370 μmol h^{-1} g^{-1}	[6]
C-PAN/CN	300 W Xe lamp, λ > 400 nm	100 mg, 3 wt% of Pt co-catalyst, TEOA (10%)	1775 μmol h^{-1} g^{-1}	[7]
CPFA/CN	300 W Xe lamp, λ > 400 nm	100 mg, 3 wt% of Pt co-catalyst, TEOA (10%)	587.4 μmol h^{-1} g^{-1}	[8]
PDA/CN	300 W Xe lamp, λ > 420 nm	50 mg, 3 wt% of Pt co-catalyst, TEOA (10%)	1380 μmol h^{-1} g^{-1}	[9]
PTEtOH/CN	300 W Xe lamp, λ > 420 nm	100 mg, 1 wt% of Pt co-catalyst, TEOA (10%)	1518.2 μmol h^{-1} g^{-1}	[10]

PEDOT/CN	300 W Xe lamp, λ > 400 nm	100 mg, 1 wt% of Pt co-catalyst, TEOA (10%)	327 μmol h^{-1} g^{-1}	[11]
PP_y/CN	300 W Xe lamp, λ > 400 nm	100 mg, 3 wt% of Pt co-catalyst	154 μmol h^{-1} g^{-1}	[12]
PFO/CN	300 W Xe lamp, λ > 420 nm	100 mg, 1 wt% of Pt co-catalyst, TEOA (10%)	513.4 μmol h^{-1} g^{-1}	[13]

Reference:

[1] H. Zhang, Z. Liu, J. Fang and F. Peng, Modulation of π-Electron Density in Ultrathin 2D Layers of Graphite Carbon Nitride for Efficient Photocatalytic Hydrogen Production, *Small,* 2024, 2404929.

[2] X. Zhong, Y. Zhu, Y. Wang, Z. Jia, M. Jiang, Q. Sun and Jianfeng Yao, Intramolecular Quaternary Carbon Nitride Homojunction for Enhanced Visible Light Hydrogen Production, *Small,* 2024, 2402219.

[3] Z. Zhang, L. Ren, H. Li, D. Jiang, Y. Fang, H. Du, G. Xu, C. Zhu, H. Li, Z. Lu and Y, Yuan, π-Conjugated In-Plane Heterostructure Enables Long-Lived Shallow Trapping in Graphitic Carbon Nitride for Increased Photocatalytic Hydrogen Generation, *Small,* 2023, 2207173.

[4] F. Yin, P. Qin, J. Xu and S. Cao, Methylene Blue Incorporated Donor-Acceptor g-C_3N_4 Nanosheet Photocatalyst for H_2 Production, *Acta Phys. -Chim. Sin.*, 2023, **39**, 2212062.

[5] C. D. Windle, A. Wieczorek, L. Xiong, M. Sachs, C. Bozal-Ginesta, H. Cha, J. K. Cockcroft, J. Durrant and J. Tang, Covalent grafting of molecular catalysts on $C_3N_xH_y$ as robust, efficient and well-defined photocatalysts for solar fuel synthesis, *Chem. Sci.*, 2020, **11**, 8425.

[6] F. He, G. Chen, Y. Yu, S. Hao, Y. Zhou and Y. Zheng, Facile approach to synthesize g-PAN/g-C_3N_4 composites with enhanced photocatalytic H_2 evolution activity. *ACS Appl. Mater. Interface*, 2014, **6**, 7171-7179.

[7] F. He, G. Chen, J. Miao, Z. Wang, D. Su, S. Liu, W. Cai, L. Zhang, S. Hao and B. Liu, Sulfur-mediated self-templating synthesis of tapered C-PAN/g-C_3N_4 composite nanotubes toward efficient photocatalytic H_2 evolution. *ACS Energy Lett.*, 2016, **1**, 969-975.

[8] W. Xing, C. Li, Y. Wang, Z. Han, Y. Hu, D. Chen, Q. Meng and G. Chen, A novel 2D/2D carbonized poly-(furfural alcohol)/g-C_3N_4 nanocomposites with enhanced charge carrier separation for photocatalytic H_2 evolution. *Carbon*, 2017, **115**, 486-492.

[9] P. Xia, M. Liu, B. Cheng, J. Yu and L. Zhang, Dopamine modified g-C_3N_4 and its enhanced visible-light photocatalytic H_2-production activity. *ACS Sustain. Chem. Eng.*, 2018, **6**, 8945-8953.

[10] Q. Zhao, Y. Li, K. Hu, X. Guo, Y. Qu, Z. Li, F. Yang, H. Liu, C. Qin and L. Jing, Controlled synthesis of nitro-yerminated poly[2-(3-thienyl)-ethanol]/g-C_3N_4 nanosheet heterojunctions for efficient visible-light photocatalytic hydrogen evolution. *ACS Sustain. Chem. Eng.*, 2021, **9**, 7306-

7317.
[11] Z. Xing, Z. Chen, X. Zong and L. Wang, A new type of carbon nitride-based polymer composite for enhanced photocatalytic hydrogen production. *Chem. Commun.*, 2014, **50**, 6762-6764.
[12] Y. Sui, J. Liu, Y. Zhang, X. Tian and W. Chen, Dispersed conductive polymer nanoparticles on graphitic carbon nitride for enhanced solar-driven hydrogen evolution from pure water. *Nanoscale*, 2013, **5**, 9150-9155.
[13] J. Chen, C. Dong, D. Zhao, Y. Huang, X. Wang, L. Samad, L. Dang, M. Shearer, S. Shen and L. Guo, Molecular design of polymer heterojunctions for efficient solar-hydrogen conversion. *Adv. Mater.*, 2017, **29**, 1606198.